ELSEVIER

NeuroImage

www.elsevier.com/locate/ynimg
NeuroImage 41 (2008) 525–534

Modeling of region-specific fMRI BOLD neurovascular response functions in rat brain reveals residual differences that correlate with the differences in regional evoked potentials

Christopher P. Pawela,[a] Anthony G. Hudetz,[b] B. Douglas Ward,[a] Marie L. Schulte,[b] Rupeng Li,[a] Dennis S. Kao,[c] Matthew C. Mauck,[d] Younghoon R. Cho,[c] Jay Neitz,[d] and James S. Hyde[a,*]

[a]*Department of Biophysics, Medical College of Wisconsin, 8701 Watertown Plank Road, Milwaukee, WI 53226, USA*
[b]*Department of Anesthesiology, Medical College of Wisconsin, 8701 Watertown Plank Road, Milwaukee, WI 53226, USA*
[c]*Department of Plastic Surgery, Medical College of Wisconsin, 8701 Watertown Plank Road, Milwaukee, WI 53226, USA*
[d]*Department of Cell Biology, Neurobiology, and Anatomy, Medical College of Wisconsin, 8701 Watertown Plank Road, Milwaukee, WI 53226, USA*

Received 18 October 2007; revised 18 January 2008; accepted 19 February 2008
Available online 4 March 2008

The response of the rat visual system to flashes of blue light has been studied by blood oxygen level-dependent (BOLD) functional magnetic resonance imaging (fMRI). The BOLD temporal response is dependent on the number of flashes presented and demonstrates a refractory period that depends on flash frequency. Activated brain regions included the primary and secondary visual cortex, superior colliculus (SC), dorsal lateral geniculate (DLG), and lateral posterior nucleus (LP), which were found to exhibit differing temporal responses. To explain these differences, the BOLD neurovascular response function was modeled. A second-order differential equation was developed and solved numerically to arrive at region-specific response functions. Included in the model are the light input from the diode (duty cycle), a refractory period, a transient response following onset and cessation of stimulus, and a slow adjustment to changes in the average level of the signal. Constants in the differential equation were evaluated for each region by fitting the model to the experimental BOLD response from a single flash, and the equation was then solved for multiple flashes. The simulation mimics the major features of the data; however, remaining differences in the frequency dependence of the response between the cortical and subcortical regions were unexplained. We hypothesized that these discrepancies were due to regional-specific differences in neuronal response to flash frequency. To test this hypothesis, cortical visual evoked potentials (VEPs) were recorded using the same stimulation protocol as the fMRI. Cortical VEPs were more suppressed than subcortical VEPs as flash frequency increased, supporting our hypothesis. This is the first report that regional differences in neuronal activation to the same stimulus lead to differential BOLD activation.

Keywords: Visual system; BOLD signal; Rat brain fMRI; Neuronal adaptation; Hemodynamic response modeling; Visual evoked potentials

* Corresponding author. Fax: +1 414 456 6512.
E-mail address: jshyde@mcw.edu (J.S. Hyde).
Available online on ScienceDirect (www.sciencedirect.com).

1053-8119/$ - see front matter © 2008 Elsevier Inc. All rights reserved.
doi:10.1016/j.neuroimage.2008.02.022

Introduction

Since the introduction of blood oxygen level-dependent (BOLD) functional magnetic resonance imaging (fMRI) (Ogawa et al., 1990) and its subsequent demonstration in humans (Bandettini et al., 1992; Kwong et al., 1992; Ogawa et al., 1992), there have been efforts to determine the coupled effect of neuronal activity and vascular hemodynamics on the observed BOLD response. Major efforts have been made through experimental methods to tie BOLD signal changes to either neuronal spiking frequency (Hyder et al., 2002) or local field potentials (Logothetis et al., 2001). Modeling the neurovascular response function is now a major line of research (Buxton et al., 1998; Friston et al., 2000). The purpose of a model is to establish differences based on certain assumptions. Most stimuli cause event-related changes in neuronal activity, which can be used to model the effect on the BOLD signal (David et al., 2005; Friston et al., 1998). A major unresolved question is whether there are differences in BOLD signals arising from the different structures in the visual pathway. To answer this question, we measured and modeled the BOLD neurovascular response function in various regions of the rat visual system caused by retinal stimulation with diffuse 465-nm-flashing light-emitting diodes (LEDs). The model accounted for some, but not all, of the observed differences across the various regions. We tested the hypothesis that variations of regional-specific neuronal inputs as determined by visual evoked potentials (VEPs) account for apparent failures of the model. Data are presented that support the hypothesis.

Light striking the retina generates activity that is processed both hierarchically and parallel by the visual system (Felleman and Van Essen, 1991). Diverse populations of ganglion cells project retinal activity to the superior colliculus (SC) and relay nuclei in the thalamus, notably the dorsal lateral geniculate (DLG), ventral lateral geniculate

(LGv), and lateral posterior nucleus (LP) (Boka et al., 2006; Li et al., 2003). The DLG projects to the primary visual cortex (VISp), defined as V1 in the Paxinos atlas (Paxinos and Watson, 2005), while the SC via the LP projects to other cortical areas [posterior lateral visual area (VISpl), posterior medial visual area (VISpm), and probable visual area (VISx), all defined as V2 in the Paxinos atlas (Paxinos and Watson, 2005)].

Previous studies have shown that the visual cortex and SC respond to on/off stimuli in rodents (Cooper and Thurlow, 1991; Cooper et al., 1991), including one recent fMRI study in rats (Van Camp et al., 2006a). The BOLD impulse response to short visual stimuli of varying frequency has been previously measured and modeled in human visual cortex (Janz et al., 2001). In this work, we observe and model the temporal changes in measured BOLD signal in various cortical V1/V2 and subcortical DLG, SC, and LP structures in rat brain.

It has been shown that the BOLD response to stimuli is nonlinear (Birn et al., 2001; Friston et al., 1998). The event-related BOLD signal has been found to be highly dependent on the fraction of time the stimulus is on, also known as the duty cycle of the stimulus (Birn and Bandettini, 2005). Birn and Bandettini explored the effect a modulated neuronal input has on the Buxton balloon hemodynamic model (Buxton et al., 1998). Effects that were modeled included the duty cycle of the stimulus, neuronal adaptation (the decay in response to repetitive stimulation), a stimulus "off" response, and a neuronal refractory period (recovery from adaptation after stimulus cessation). The refractory properties of sensory systems, such as the visual system described by Birn and Bandettini, are suitable for modeling BOLD responses. In this work, we modeled BOLD neurovascular response functions observed throughout the rat visual system when stimulated with short (5 ms) duration, flashing 465-nm light over a range of frequencies.

We hypothesized that the physiological process governing the BOLD response to LED flashes at different frequencies can be modeled by solutions to a differential equation developed as follows: The system input is modeled as a variable duty cycle light source, and a neuronal refractory period following the stimulation period is introduced to describe the transient nature of retinal ganglion cell responses to repetitive changes in field luminance. A transient response follows the onset and cessation of the stimulus combined with the adaptation gain modeled as an adjustment to change in the average level of the signal. The underlying process in this last step could be neuronal in origin or physical, such as a ceiling to possible increase in blood flow. These steps lead to a differential equation that contains a number of variables. These are set for each brain region by measuring the response to a single 5-ms light flash, and the differential equation is solved numerically for every input. A specific BOLD neurovascular response function is obtained for each region for each flash frequency.

Differences between experiment and model were observed in the five visual-system brain regions that were studied. We tested whether or not those residual differences correlate with differences in VEPs.

Materials and methods

fMRI animal preparation

All procedures and protocols were in compliance with the Medical College of Wisconsin's Institutional Animal Care and Use Committee. Five male Sprague-Dawley rats (Charles River Laboratories, Wilmington, MA) were initially anesthetized with 2.5% isoflurane and placed supine on a heated surgical table. Isoflurane was reduced to 1.5% for maintenance. The right femoral artery and vein were cannulated for experimental access with PE-50 tubing (Stoelting, Wood Dale, IL). A tracheostomy was performed for mechanical ventilation during the fMRI protocol. The animal was then placed in a custom-built G-10 fiberglass rodent cradle for imaging. G-10 fiberglass was used because it has a magnetic susceptibility similar to air. The animal was ventilated using an MRI-compatible ventilator (MRI-1; CWE, Ardmore, PA). End-tidal gases were monitored (POET-IQ2; Criticare Systems, Waukesha, WI), and the respiratory rate was maintained between 55 and 65 breaths per minute depending on the end-tidal CO_2 reading. The animal's core temperature was sustained at 37 °C by a recirculating water pump (Meditherm-III; Gaymar Industries, Orchard Park, NY). Invasive blood pressure (Model 1025; SA-Instruments, Stony Brook, NY) and pulse oximetry (Model 8600V; Nonin Medical, Plymouth, MN) were monitored throughout the course of the experiment. All physiologic parameters were recorded by a computer (Windaq Pro; DataQ Instruments, Akron, OH). A 0.1-mg/kg/h infusion of medetomidine hydrochloride (Domitor; Pfizer Animal Health, New York, NY) anesthesia with 2-mg/kg/h pancuronium bromide (Hospira Inc., Lake Forest, IL) was started and isoflurane was ended. An MRI-compatible infusion pump (Harvard Apparatus, Boston, MA) was used. Albino rats were used because they have a transparent nictitating membrane, and, therefore, their pupil does not need to be dilated with atropine. Kimura (1962) also compared albino and Long-Evans rats and found no difference in the photic evoked responses between the two. Spectral radiance was measured with the LED placed 2 cm from the probe by a spectroradiometer (RPS 380; International Light Technologies, Peabody, MD).

fMRI protocol

All experiments were performed in a Bruker 9.4 T (AVANCE, Billerica, MA) small-animal scanner. Two blue MRI-compatible LEDs with a wavelength of 465 nm were placed bilaterally 2 cm from both eyes of the rat. The LEDs were computer-controlled (Labview Software; National Instruments, Austin, TX) and triggered by a Transistor–Transistor Logic (TTL) pulse from the scanner. The lights in the scanner suite were turned off, and the rat was allowed to rest for 20 min to become "dark-adapted." An initial rapid acquisition with relaxation enhancement (RARE) anatomic image set was acquired followed by two resting-state scans with no stimulus (no light). For the fMRI stimulation experiments, a boxcar paradigm was used with an initial 40-s off period followed by three on/off cycles (20 s on/40 s off) for a total of 3 min 40 s. During the three 20-s stimulation periods, the LEDs were flashed at frequencies of 0.1 (2 flashes), 0.2 (4 flashes), 1 (20 flashes), 5 (100 flashes), or 10 Hz (200 flashes). Each flash had a constant duration of 5 ms. Fifteen experiments were performed on each rat; five stimulation parameters were used (0.1, 0.2, 1, 5, and 10 Hz) for the left or right eye as well as bilaterally. A 10-min rest period was included between scans allowing the animal to return to the "dark-adapted" condition. The total experiment time was between 3.5 and 4 h.

MRI parameters

All scans were acquired with 15 contiguous 1-mm slices; the third slice was located over the anterior commissure centered −0.36 mm from bregma. The RARE anatomy was obtained with a 256×256 matrix, TE=50.8 ms, and FOV=35 mm. The EPI parameters were

96×96 (zero-filled to 128×128), TR=2 s, TE=18.76 ms, FOV=35 mm, and 110 repetitions for a total scan time of 3 min 40 s.

fMRI analysis

All EPI acquisitions were first registered using FMRIB's Linear Image Registration Tool (FLIRT) (Jenkinson et al., 2002) to an "ideal" anatomy chosen from the experimental dataset. Further analysis was carried out using the Analysis of Functional NeuroImages (AFNI) software suite (Cox and Hyde, 1997). The five experiments for each stimulation condition were averaged together with AFNI, 3dcalc. These averaged EPI datasets were used to create activation maps by performing an *F*-test on the time series data using the design block as the only regressor (AFNI, 3dDeconvolve). A *p*-value of 0.005 was used for plotting and was the activation threshold. All activation maps were overlaid on the "ideal" RARE anatomy used in the registration process. Regions of interest (ROI) were drawn for the five brain regions used in the analysis (V1, V2, DLG, SC, and LP) (Paxinos and Watson, 2005). The time series for all active voxels in each region were averaged.

BOLD hemodynamic modeling

The neuronal "refractory period" was modeled by an exponential decay following the most recent visual stimulus. The refractory gain can be written as:

$$g(t) = 1 - \exp(-\alpha(t - t_0)) \tag{1}$$

where t_0=time of most recent visual input stimulus and α is the exponential decay rate. The model parameter α was set equal to $1/\tau_\alpha$, where τ_α=5 s (Birn and Bandettini, 2005). The effect of the refractory period on the signal was modeled as the product of the visual input stimulus with the refractory gain:

$$z(t) = g(t)s(t) \tag{2}$$

where $s(t)$ represents the visual input stimulus as a function of time t. That is, $s(t)$ is "1" for each 5 ms epoch of visual stimulus and "0" otherwise. Next, we modeled the transient of neural activity following onset of a stimulus, as well as the transient following stimulus cessation, using a first-order differential equation; specifically,

$$\tau_f \mathrm{d}f(t)/\mathrm{d}t + f(t) = z(t) \tag{3}$$

where $f(t)$=transient response, and τ_f=time constant for this first-order system. The model parameter τ_f was set equal to 0.5 s, in accordance with the "off response" decay time (Birn and Bandettini, 2005).

Next, we modeled "adaptation" as a slow adjustment to changes in the average level of the signal. The estimate of the current mean signal level $m(t)$ was modeled as a first-order differential equation:

$$\tau_m \mathrm{d}m(t)/\mathrm{d}t + m(t) = f(t) \tag{4}$$

where τ_m=time constant for this first-order system. The model parameter τ_m was set equal to 25 s. We hypothesized that the system adjusted to long-term changes in the average signal level. That is, if the above $m(t)$ represents the "predicted" or "baseline" signal level, then $f(t)-m(t)$ represents change relative to baseline. For convenience, let:

$$u(t) = f(t) - m(t) \tag{5}$$

Next, the BOLD neurovascular response function was modeled, for each region, as the solution to a linear second-order differential equation:

$$\mathrm{d}^2y(t)/\mathrm{d}t^2 + 2\zeta\omega_n \mathrm{d}y(t)/\mathrm{d}t + \omega_n^2 y(t) = \omega_n^2 \kappa\, u(t - \tau_d) \tag{6}$$

where

$y(t)$=BOLD response (function)
κ=constant scale factor relating input to output
τ_d=time delay of initial hemodynamic response relative to neuronal input(s)
ζ, ω_n=constants describing "shape" of the BOLD neurovascular response function

The array of model parameters $\boldsymbol{\theta}=[\kappa\ \tau_d\ \zeta\ \omega_n]$ was estimated individually for each region of interest using the data from the first (0.1 Hz) input paradigm only. To estimate these parameters, we used the Matlab implementation of the Nelder–Mead simplex algorithm for nonlinear parameter optimization, with additional constraints on some of the unknown parameters. Specifically, the "shape" parameters ζ and ω_n were constrained to lie within 20% of the nominal values for the assumed canonical BOLD neurovascular response function. This incorporates the common assumption that the shape of the BOLD response is essentially similar across brain regions.

Procedures for VEPs

Five male Sprague-Dawley rats (333±40 g SD) kept on a reversed light–dark cycle were anesthetized for surgery with 1.4% isoflurane (Abbot Laboratories, Chicago, IL) vaporized into O_2/N_2 (30%/70%). Body temperature was sustained at 37 °C with a water-circulating heating pad (Gaymar Industries, Orchard Park, NY). The femoral arteries and veins were catheterized for the measurement of arterial blood pressure and gases. All incisions were liberally coated with 1% xylocaine gel, a topical local anesthetic. Rats were tracheostomized and ventilated.

Heads were secured in a stereotaxic apparatus (Kopf Instruments, Tujunga, CA). A 1.5-mm-wide, 3-mm-long slit of the cranium, above the right primary visual cortex and SC, −6.6 mm caudal, and centered at +2.5 mm lateral from bregma, was bilaterally thinned to translucency. Tripolar electrodes (M333; Plastics One, Roanoke, VA) were cut to length to target the SC and the intragranular layers of V1. The reference electrode was in the superficial cortex. The electrodes were inserted using micromanipulators. Following the placement of the electrodes, infusion of a mixture of 0.1 mg/kg/h medetomidine hydrochloride (Domitor; Pfizer Animal Health) and 2.0 mg/kg/h pancuronium bromide (Hospira Inc.) was started (Syringe Pump Model 22; Harvard Apparatus, Holliston, MA), and the isoflurane was gradually tapered to zero over several minutes. About 15 to 20 min after the medetomidine/pancuronium infusion started, the arterial blood was sampled for dissolved gases and pH. Then, the first set of stimulation blocks was bilaterally presented to the eyes of the rat.

Bilateral visual stimulation was produced using the same apparatus as used in the MR suite. It consisted of trains of flashes

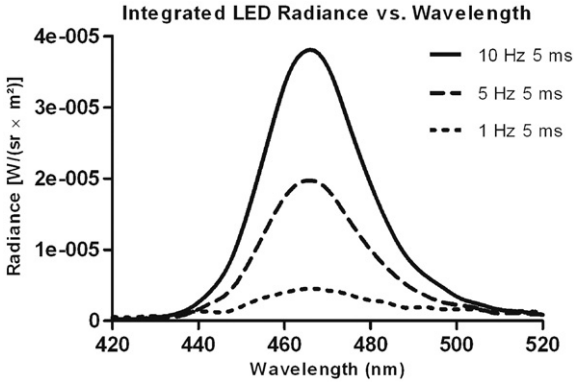

Fig. 1. Integrated spectral radiance of the blue LED at a fixed pulse width of 5 ms. Several different flash frequencies are plotted (1, 5, and 10 Hz). Note the linearity of the response with increasing flash rate.

with a pulse width of 5 ms and a frequency that varied between 0.1, 0.2, 1, 5, and 10 Hz. The standard block design protocol consisted of three blocks of 40 s of rest followed by 20 s of rest at each frequency. Approximately 3 min 40 s elapsed between each frequency application. The frequencies were presented in random order.

Mean arterial blood pressure (MAP), stimulation timing signals, and VEPs were digitally sampled at 1000 Hz (WinDaq; DataQ Instruments) and were recorded on a PC. Inspired and expired gases were continuously monitored with an online gas analyzer (POET-IQ2; Criticare Systems). VEP data from V1 and the SC were analyzed using Matlab (Mathworks, Natick, MA). VEPs were extracted by averaging local field potentials from 100 to 300 flash trials. The maximum amplitude of the middle latency components of VEP was measured by taking the difference between the first major positive peak near 40 ms post-stimulus and the subsequent minimum value reached before the next zero crossing (from negative to positive) of the signal. Although the VEP waveform and latency varied slightly with repeating block trials and various flash frequencies, in all cases the measured positive–negative wave was within the first 100 ms after flash.

Results

Spectral radiance

To validate that the LED flash intensity is stable over the frequency domain, we measured the spectral radiance. Fig. 1 shows plots of the integrated radiance from the LED system vs. wavelength. The radiance was measured over a period of 2 s. The integrated radiance was determined to be linear with increasing flash frequency, confirming that the stimulus performed as expected. The maximum radiance was at 465 nm, falling within the blue range in the visual spectrum. The LEDs used in this study were chosen because they were used in a previous fMRI study of rabbit vision (Wyrwicz et al., 2000). It was also determined that the evoked potentials were not different between blue and green LEDs (unpublished data).

fMRI BOLD response to binocular stimulation

Average activation maps for bilateral 0.1 Hz flash frequency are shown in Fig. 2. The 1-mm slices are located −4.36 to −9.36 mm from bregma. The major structures for the two main pathways involved in visual transduction are located within these slices. The DLG, LP, SC, V1, and V2 are clearly discernible and labeled on

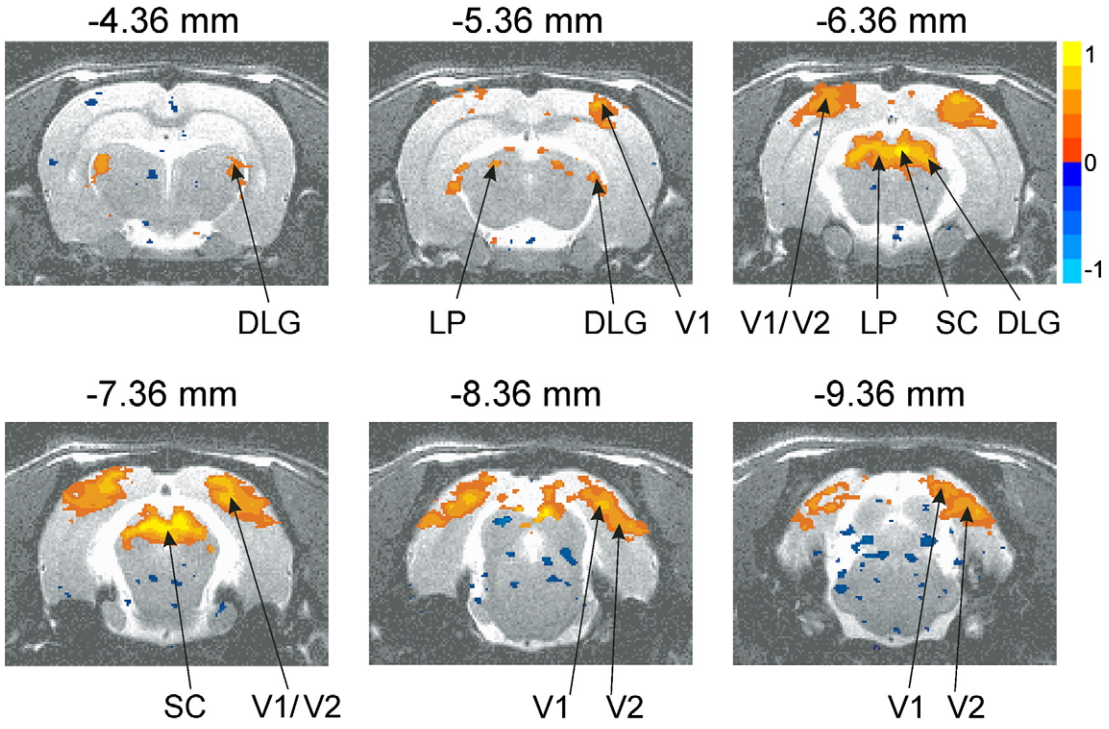

Fig. 2. Activation map of BOLD response to 0.1 Hz flash rate in a series of 1 mm contiguous slices in rat brain. The results from five animals were averaged. The first slice plotted (top left) is centered −4.36 mm from bregma, with the final slice centered −9.36 mm (bottom right) from bregma. Structures activated include the DLG, LP, SC, V1, and V2. Task activation is overlaid on the RARE anatomy. See the Introduction for abbreviations.

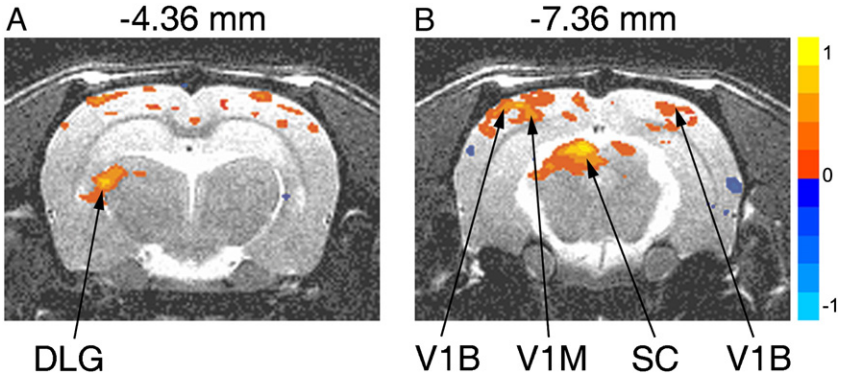

Fig. 3. BOLD activation map resulting from single right-side flashing at a frequency of 10 Hz. Two 1-mm slices are plotted, located either −4.36 mm (left) or −7.36 mm (right) from bregma. Activation in the left slice occurred in the contralateral DLG with some diffuse activation in the cortex. Activation in the right slice included response in the contralateral SC, contralateral V1M, and ipsi/contralateral V1B. See the Introduction for abbreviations.

the figure. Robust activation is observed in the visual cortex with the SC displaying the strongest change in BOLD signal. The activation maps conform to the rat atlas (Paxinos and Watson, 2005) which was determined through histological and electrophysiological means. Our results extend earlier fMRI studies on the rodent visual system (Huang et al., 1996; Van Camp et al., 2006a).

fMRI BOLD response to monocular stimulation

Activation by flash to either the right or left eye shows that responses are localized to the contralateral hemisphere as expected. Response occurs primarily in the hemisphere contralateral to the stimulus in the subcortical regions such as the SC, LP, and DLG.

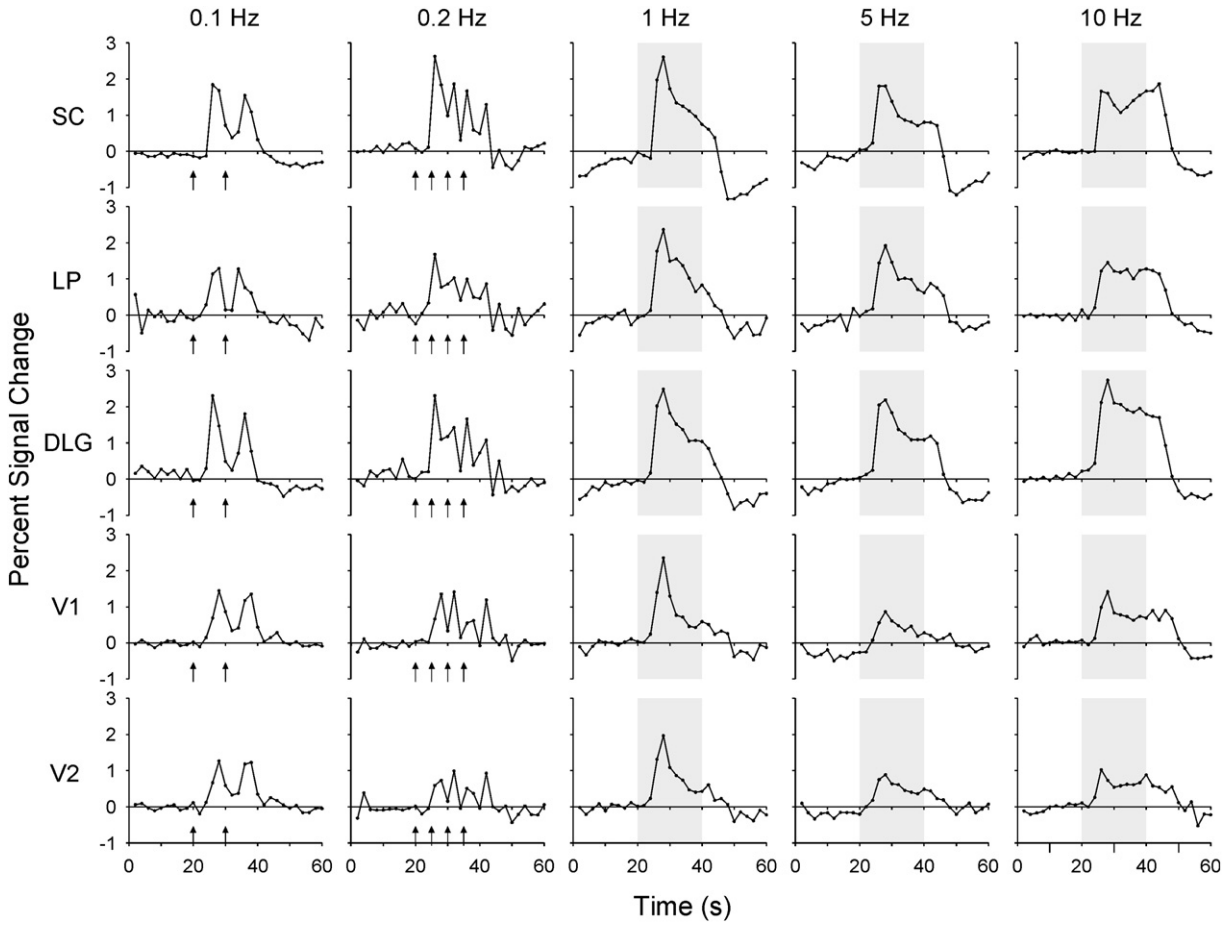

Fig. 4. Average percent signal changes in the BOLD time courses for the various structures within the rat visual system as a function of increasing flash frequency. Plotted are the SC, LP, DLG, V1, and V2. The gray area indicates the stimulus on period. Arrows are plotted at the 0.1- and 0.2-Hz frequencies displaying exact flash timing. See the Introduction for abbreviations.

Maps from one of these experiments are displayed in Fig. 3. In this experiment, light flashing at 10 Hz was presented to the right eye, and most of the resulting activation is evident on the contralateral left side in both the SC and DLG regions. As a result of overlapping visual fields, binocular areas of visual cortex are activated bilaterally in response to monocular stimulation.

Temporal BOLD response to visual stimulation

The average BOLD signal response for bilateral stimulation at different frequencies is plotted in Fig. 4. Only voxels above the *p*-value threshold of 0.005 were used in computing the averaged response for each region. The arrows displayed on the plots for 0.1 and 0.2 Hz show the timing of the flash for those two frequencies. Arrows are not displayed for the higher frequencies because of the higher flash count for the higher levels: 1 (20 flashes), 5 (100 flashes), and 10 Hz (200 flashes). Two peaks at 0.1 Hz are the result of the two flashes, and four peaks at 0.2 Hz are the result of the four flashes in all regions. In all regions, at 1 Hz and above, the response coalesces due to the slow BOLD response. After the initial peak, the response decays with repeated stimulation within each block. Following the decay, at the higher flashing rates of 5 and 10 Hz, a plateau is seen in the waveform, especially at a 10-Hz frequency.

The BOLD response is variable among the different regions along the visual pathway. The cortical signals (V1 and V2) display a more transient response than subcortical regions (DLG/LP/SC). This signal attenuation in the cortex vs. the subcortex was the major focus of this study. There appears to be a slightly longer delay in the BOLD impulse response for the cortical regions compared to the subcortical structures. There is a significant "off" response visible as a second peak at 1 to 10 Hz in the SC and DLG following stimulus cessation. The post-stimulus undershoot is also more pronounced in the subcortical structures (DLG/LP/SC) than in V1/V2, especially at the higher frequencies from 1 to 10 Hz.

Modeling BOLD impulse response

The visual input stimulus $s(t)$ is displayed in row (a) of Fig. 5 for the five different experimental designs labeled "0.1 Hz" through "10 Hz". Note that as the frequency increases the *duty cycle* increases. That is, the duty cycle varied from 0.0005 to 0.05, or a range of 100 to 1. This large variation in the nature of the stimulus revealed major nonlinearity in the system response, as indicated in Fig. 4. For example, the individual visual pulses can be resolved from the fMRI signal at 0.1 and 0.2 Hz; however, the individual pulses cannot be resolved at 1 Hz or higher. Indeed, although the input signal power increased by almost a factor of 10 over the 1- to

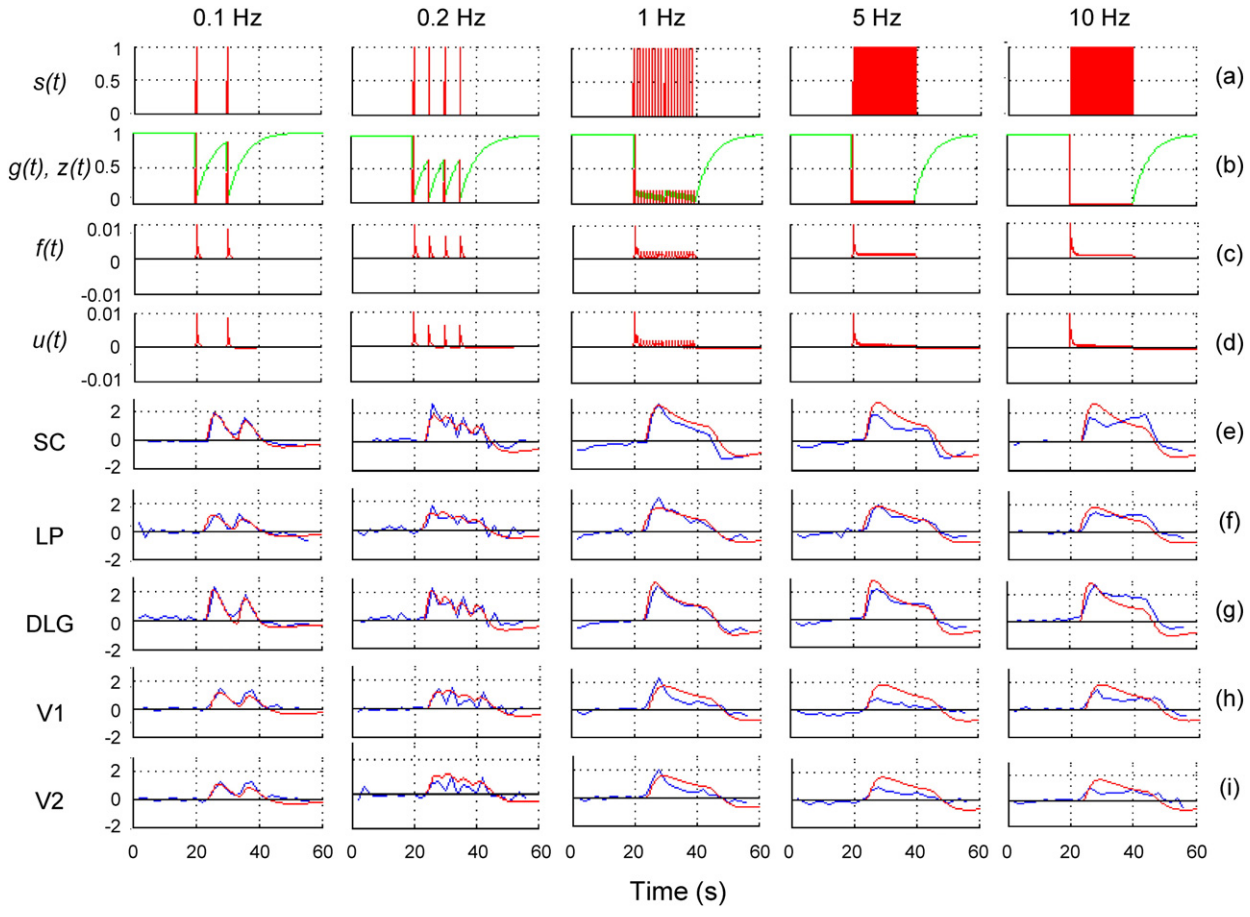

Fig. 5. The five columns correspond to the five different visual input stimulus patterns (0.1 to 10 Hz). The rows correspond to: (a) visual input stimulus $s(t)$; (b) modeled refractory gain $g(t)$ (green curve) and refractory signal $z(t)$ (red curve); (c) transient signal $f(t)$; (d) modeled neuronal input signal $u(t)$ resulting from light adaptation, representing common neuronal input to all ROIs; and (e) through (i) measured (blue) and modeled (red) BOLD signal for the five regions.

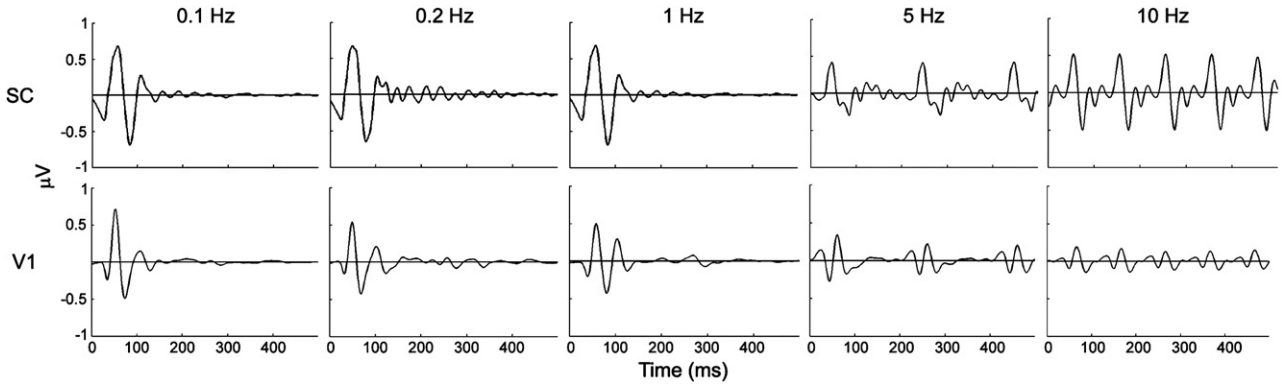

Fig. 6. VEPs measured in the superior colliculus (SC) and primary visual cortex (V1) as a function of frequency. The amplitudes of the evoked responses are plotted in millivolts (y-axis) and the timing in milliseconds. Note the sampling rate (1 kHz) of the VEPs are much faster than the sampling rate of the fMRI (TR = 2 s).

10-Hz range, the amplitude of the measured response was relatively constant, indicative of a nonlinear system.

The nonlinearity was modeled, as described in the Methods section, by an exponential decay representing the neuronal "refractory period." The result from applying Eq. (1) is the refractory gain function $g(t)$, illustrated by the green curves in row (b) of Fig. 5. Here, we used a fixed decay rate of $\alpha = 0.20\ s^{-1}$ (Birn and Bandettini, 2005). The red curves in row (b) represent the refractory signal; that is, the refractory signal $z(t)$ is obtained as the product (see Eq. (2)) of the gain function $g(t)$ and the input stimulus function $s(t)$ from row (a).

The transient response $f(t)$ was modeled using Eq. (3) and is plotted in row (c) of Fig. 5. Note that $f(t)$ is a slightly smoothed version of $z(t)$. The local mean signal level $m(t)$ was calculated using Eq. (4), with integration time constant $\tau_m = 25$ s. The adaptation signal was then calculated as the difference $u(t) = f(t) - m(t)$ (Eq. (5)) and is displayed in row (d) of Fig. 5.

Using the Nelder–Mead simplex algorithm for nonlinear least squares optimization, the model parameter array $\boldsymbol{\theta} = [\kappa\ \tau_d\ \zeta\ \omega_n]$, subject to the parameter constraints, was fitted to the data from each row and the first column of Fig. 4 by numerical solution of Eq. (6) separately for each region. The results are displayed in rows (e) through (i) of Fig. 5, where the fitted estimate of the normalized BOLD response $y(t)$ (red curve) is superimposed on the fMRI data (blue curve).

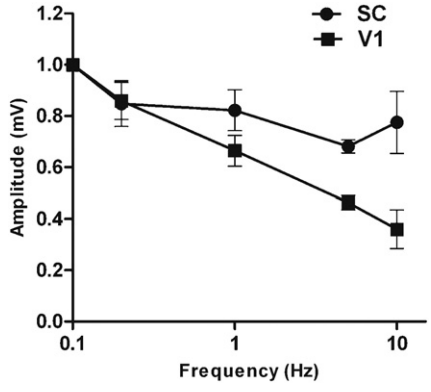

Fig. 7. Normalized mean peak-to-peak VEPs plotted as a function of frequency. The results are plotted for both the primary visual cortex (V1) and the superior colliculus (SC). The standard error of the mean is included in the graph for each point.

The model is able to reproduce most of the major features of the experimental data. However, the model was unable to reproduce the suppressed response in the cortex when compared to the subcortical structures. Compare rows (h) and (i) of Fig. 5 with rows (e), (f), and (g). We hypothesize that the differences were due to some unknown neuronal input that was not included in the model. The model also failed to mimic the off-response that occurs mainly in the SC.

Visual evoked potentials

The differences between the V1 and SC were investigated further by measuring the VEPs in each region with the same stimulus used in the fMRI experiments. Fig. 6 displays the measured VEPs in response to flash as a function of stimulus frequency in one experiment as an example. The amplitude of the response decreases with increasing frequency in the V1 when compared to the SC. The normalized mean peak-to-peak evoked potentials from all experiments are summarized in Fig. 7. The differences in evoked potentials between the two regions are statistically significant at 1, 5, and 10 Hz but were not at 0.1 and 0.2 Hz when tested with a paired t-test with 95% confidence intervals. These results are consistent with the hypothesis that the regional differences in observed BOLD response with increasing stimulation frequency are due to regional differences in neuronal activation.

Discussion

The goal of our investigation was to understand the frequency dependence of the BOLD response to light flashes in the different areas of the rat visual system. Mathematical modeling of the BOLD signal replicates observed regional differences fairly well. The residual differences between the experimental BOLD signals and the neurovascular response function model developed here appear to arise from a failure to include in sufficient detail all variations in neuronal inputs that occur because of change in flash frequency. Separate VEP experiments are consistent with this hypothesis.

The rat has relatively large subcortical structures in the visual system (i.e., the DLG, LP, and SC) compared to human brain, which makes it ideally suited for this work. Our LED experimental setup permits study not only of the rodent visual system but also of the dynamics of the BOLD signal. Much of the fMRI literature in the human brain has focused on the cortex due to its relatively large

size and complexity. This study took advantage of higher field strength (9.4 T) and corresponding smaller voxel size to study the often overlooked subcortical visual areas.

Localization of BOLD response

As seen in Fig. 2, binocular LED flashes (0.1 Hz) activated all of the structures in the visual pathway. Rats have relatively small overlapping visual fields, allowing the primary visual cortex (V1) to be divided functionally into monocular (V1M) and binocular (V1B) zones (Fig. 3) by selectively flashing either the right or left eye. LED stimulus produced a robust BOLD response even at short 5-ms pulse widths. Previous studies in rodents did not report the visually activated thalamic sites that represent important relay sites to both the SC and cortex (Huang et al., 1996; Van Camp et al., 2006a). The activation of the DLG by flash stimuli is a novel aspect of this study.

We also extended testing to lower frequencies (0.1 and 0.2 Hz) in comparison with previous investigations (Van Camp et al., 2006a). Low frequencies are important because they allow the full expression of neuronal response to flash. An inter-stimulus-interval (ISI) shorter than 5 s does not allow full recovery. We also demonstrated the BOLD response to increasing discrete flash frequencies without the need to pool the data into frequency ranges. We suppose that the advantage of a higher field (9.4 T) contributed to this success.

Dynamics of the BOLD response

The BOLD response to repeated flashes, as shown in Fig. 4, has both similarities and differences across cortical and subcortical structures. The hemodynamic delay seems to be relatively constant across subcortical regions (DLG/LP/SC): around 4 to 6 s with a slight delay for the cortex (V1/V2). The maximum peak height was obtained 6 to 8 s after initial stimulation. However, our repetition time (T_R) was 2 s, limiting our temporal resolution. There are also some major dissimilarities across the data. The BOLD response in the visual cortex (V1/V2) was attenuated when compared to the SC and DLG regions. We hypothesize two possible reasons. One is that the variable response could be a result of different microcirculation architecture among neural structures of the brain. It has been shown that the thalamic nuclei (DLG/LP) have dissimilar venous structures relative to the cortex (Paxinos, 2004). Yacoub et al. (2006) showed that the post-stimulus undershoot is sensitive to these differences in vascular architecture. The post-stimulus undershoot comparing the DLG/SC/LP and the V1/V2 regions shows significant differences, validating our variable microvasculature suggestion. The second possible reason for the variation is that visual cortex is tuned to respond to contrast edges and spatial detail in a scene while filtering out changes in diffuse illumination as provided by our stimulus (Hubel and Wiesel, 1959). The SC is tuned to respond more to on/off stimuli and changes in stimulation frequency (Paxinos, 2004). This results in an attenuation of the signal in the visual cortex when compared to the SC when driven at higher frequencies, which is apparent in the measured VEPs.

Although there are regional differences in the BOLD response across ROIs, there are important similarities. We see that the individual light pulses are resolvable from the BOLD response at 0.1 and 0.2 Hz, but not at 1 Hz or higher. This is consistent with a linear, low-pass system. However, if the system were linear, the amplitudes at 5 and 10 Hz would be much greater than the measured amplitudes. In fact, the peak amplitudes, across the 0.0005 to 0.05 range of duty cycle, are almost constant, suggesting a nonlinear process. Also, at 0.1 and 0.2 Hz, we see a consistent pattern of decreasing amplitude of the response to consecutive light pulses, particularly in the SC, LP, and DLG. For 1 to 10 Hz, we see an initial peak followed by a slow decay to a constant value. Finally, across the entire range of 0.1 to 10 Hz, we observe a lengthy, post-undershoot response. Our nonlinear model reproduces each of these features with high fidelity. Our model does, however, underestimate the visual response to stimulus offset after a 10-Hz stimulation, especially in the SC. This may be a result of an "off" response in brisk-transient retinal ganglion cells following high frequency stimulation (Bolz et al., 1981).

Modeling the BOLD response

It has been demonstrated previously in the rat whisker barrel that the area under the curve in MION-based CBV fMRI experiments exhibits a linear relationship with stimulus durations in the range of 2 to 32 s (Lu et al., 2005). Yesilyurt et al. (2007) found that the area of the observed response increases in a linear fashion with increasing pulse width from 0.1 to 5 ms in the human visual cortex. Their experiments support our neurovascular model by showing that the amount of energy (stimulus duration) has a linear effect on the BOLD response; additionally, their data show that the post-stimulus undershoot depends on pulse width.

Janz et al. (2001) compared fMRI and VEPs in human visual cortex using a reverse flashing checkerboard stimulus at different frequencies. They fit the BOLD hemodynamic response to a single 2-s stimulation period and then convolved a series of dirac delta functions describing the stimulus timing with this temporal fMRI impulse response function. This input was then fed into a linear transform model. The model of Janz et al. was able to predict accurately the BOLD response to ISIs below 2 s; however, when ISIs above 2 s were used, the system became more nonlinear and the model failed. They were unable to model the signal correctly even after weighting the model with the decrease in VEP amplitude that occurred with increasing stimulation frequency. These authors attributed their inability to model the system to nonlinearities brought about by neuronal adaptation. Our model accounts for these nonlinearities due to adaptation and therefore gives a better fit to the data.

Our approach contrasts with that of others (Friston et al., 2003; Riera et al., 2004) in that they model system nonlinearity as nonlinearity in the hemodynamics. We find that a significant source of nonlinearity occurs at the level of neuronal activation.

Neuronal activation and frequency

Imas et al. (2005, 2004) noted that reducing the ISI below 5 s reduces the full expression of flash-induced potentials in the rat visual cortex. This can be interpreted as a failure of neuronal excitability to recover in less than 5 s after supramaximal stimulation. This could lead to a gradual attenuation of the neuronal and BOLD responses to repeating flashes presented at rates higher than 0.2 Hz. Results reported here in visual cortex show an attenuation of the amplitude of the VEPs with increasing flash frequency agreeing with previous work (Imas et al., 2005, 2004).

The linkage between BOLD response and VEPs (Logothetis et al., 2001) has been demonstrated. It has been reported previously that there is a strong coupling between the somatosensory evoked potentials (SEP) and BOLD response with respect to stimulation frequency in the rat somatosensory forelimb region (Van Camp et al.,

2006b). This coupling has also been shown to be insensitive to the anesthetic used (Huttunen et al., 2008). Van Camp et al. (2006b) also showed that the stimulus pulse width has a direct effect on the induced BOLD and SEP response. Longer pulse width (0.3 to 10 ms) leads to a larger BOLD area of activation, a larger BOLD impulse response, and a greater SEP amplitude. The rat electrical forepaw stimulation method uses square wave pulses analogous to our LED setup.

Using simultaneous EEG and BOLD fMRI, Ogawa et al. (2000) demonstrated that a single electrical square wave pulse applied to a rat forepaw followed by another pulse applied in less than 60 ms to the contralateral forepaw suppressed both the neuronal and BOLD responses in the rat somatosensory cortex. The suppression was highly dependent on the ISI between pulses. In the present study, the stimulus was applied bilaterally and flashed in a synchronous fashion. We believe that bilateral suppression is not a problem for this study because we applied timed flashes to both sides. However, inhibition could become a problem when trying to model the BOLD response to more complex stimuli.

The importance of anesthesia

Success in demonstrating a robust BOLD response to flash stimulation in all major subcortical and cortical regions along the known visual pathways depends on a number of factors: a particularly important one is the proper choice of anesthetic regime. Sensory stimulation-evoked cortical responses are sensitive to anesthesia, and this sensitivity is dependent on the sensory modality (Sloan, 1998). The visual system is a favorable model because it is less prone to suppression than the somatosensory system where an anesthetic inhibition of spinal neurons severely blunts the neuronal response to peripheral sensory stimulation (Antognini and Carstens, 1998). Thus, it has been shown that flash-induced field potentials in the visual cortex of rats are preserved even in deep anesthesia achieved by various inhalational agents (Imas et al., 2005, 2004), although analogous studies with medetomidine have not been performed. In spite of preserved neuronal responsiveness, a robust visual cortical activation with fMRI in rats had been difficult to obtain (Huang et al., 1996) until Weber et al. (2006) and Van Camp et al. (2006a,b) introduced the use of alpha-2 adrenoreceptor agonist, medetomidine, for anesthesia for fMRI.

Medetomidine is an excellent sedative–anxiolytic agent with negligible ventilatory and small cardiovascular effects. In the absence of noxious stimulation, dexmedetomidine (the active enantiomer of medetomidine) suppresses the righting reflex at a relatively low plasma concentration that preserves the responsiveness of sensory neuronal pathways (Bol et al., 1999). Dexmedetomidine produces a small degree of cerebral vasoconstriction (Ganjoo et al., 1998), as opposed to the common vasodilatory effects of most anesthetics (Lee et al., 1994). As a result, dexmedetomidine (and medetomidine) does not compromise the dynamic range of the sensory stimulation-induced cerebral hemodynamic response.

Acknowledgments

This work was supported by grants EB000215, EB000215-S1, and GM56398 from the National Institutes of Health, and DABK39-03-C-0058 from the Counterdrug Technology Assessment Center, Office of National Drug Control Policy, White House. The authors thank Hanbing Lu, Edgar DeYoe, and Peter Bandettini for their helpful comments. The authors would also like to thank Abbie Amadio and Karen Hyde for manuscript editing and figure preparation.

References

Antognini, J.F., Carstens, E., 1998. Macroscopic sites of anesthetic action: brain versus spinal cord. Toxicol. Lett. 100–101, 51–58.

Bandettini, P.A., Wong, E.C., Hinks, R.S., Tikofsky, R.S., Hyde, J.S., 1992. Time course EPI of human brain function during task activation. Magn. Reson. Med. 25, 390–397.

Birn, R.M., Bandettini, P.A., 2005. The effect of stimulus duty cycle and "off" duration on BOLD response linearity. NeuroImage 27, 70–82.

Birn, R.M., Saad, Z.S., Bandettini, P.A., 2001. Spatial heterogeneity of the nonlinear dynamics in the fMRI BOLD response. NeuroImage 14, 817–826.

Boka, K., Chomsung, R., Li, J., Bickford, M.E., 2006. Comparison of the ultrastructure of cortical and retinal terminals in the rat superior colliculus. Anat. Rec. A Discov. Mol. Cell. Evol. Biol. 288A, 850–858.

Bol, C.J., Vogelaar, J.P., Mandema, J.W., 1999. Anesthetic profile of dexmedetomidine identified by stimulus–response and continuous measurements in rats. J. Pharmacol. Exp. Ther. 291, 153–160.

Bolz, J., Rosner, G., Wässle, H., 1981. Response latency of brisk-sustained (*x*) and brisk-transient (*y*) cells in the cat retina. J. Physiol. 328, 171–190.

Buxton, R.B., Wong, E.C., Frank, L.R., 1998. Dynamics of blood flow and oxygenation changes during brain activation: The balloon model. Magn. Reson. Med. 39, 855–864.

Cooper, R.M., Thurlow, G.A., 1991. [2-^{14}C]Deoxyglucose uptake in rat visual system during flashing-diffuse and flashing-pattern stimulation over a 6 log range of luminance. Exp. Neurol. 113, 79–84.

Cooper, R.M., Thurlow, G.A., Jeeva, A., 1991. Effects of flashing-diffuse light on [2-^{14}C]deoxyglucose uptake in the visual system of the black-hooded rat. Behav. Brain Res. 46, 63–70.

Cox, R.W., Hyde, J.S., 1997. Software tools for analysis and visualization of fMRI data. NMR Biomed. 10, 171–178.

David, O., Harrison, L., Friston, K.J., 2005. Modeling event-related responses in the brain. NeuroImage 25, 756–770.

Felleman, D.J., Van Essen, D.C., 1991. Distributed hierarchical processing in the primate cerebral cortex. Cereb. Cortex 1, 1–47.

Friston, K.J., Fletcher, P., Josephs, O., Holmes, A., Rugg, M.D., Turner, R., 1998. Event-related fMRI: characterizing differential responses. NeuroImage 7, 30–40.

Friston, K.J., Harrison, L., Penny, W., 2003. Dynamic causal modeling. NeuroImage 19, 1273–1302.

Friston, K.J., Mechelli, A., Turner, R., Price, C.J., 2000. Nonlinear responses in fMRI: the Balloon model, Volterra kernels, and other hemodynamics. NeuroImage 12, 466–477.

Ganjoo, P., Farber, N.E., Hudetz, A., Smith, J.J., Samso, E., Kampine, J.P., Schmeling, W.T., 1998. In vivo effects of dexmedetomidine on laser-Doppler flow and pial arteriolar diameter. Anesthesiology 88, 429–439.

Huang, W., Plyka, I., Li, H., Eisenstein, E.M., Volkow, N.D., Springer Jr., C.S., 1996. Magnetic resonance imaging (MRI) detection of the murine brain response to light: temporal differentiation and negative functional MRI changes. Proc. Natl. Acad. Sci. U. S. A. 93, 6037–6042.

Hubel, D.H., Wiesel, T.N., 1959. Receptive fields of single neurones in the cat's striate cortex. J. Physiol. 148, 574–591.

Huttunen, J.K., Grohn, O., Penttonen, M., 2008. Coupling between simultaneously recorded BOLD response and neuronal activity in the rat somatosensory cortex. NeuroImage 39, 775–785.

Hyder, F., Rothman, D.L., Shulman, R.G., 2002. Total neuroenergetics support localized brain activity: implications for the interpretation of fMRI. Proc. Natl. Acad. Sci. U. S. A. 99, 10771–10776.

Imas, O.A., Ropella, K.M., Ward, B.D., Wood, J.D., Hudetz, A.G., 2005. Volatile anesthetics enhance flash-induced gamma oscillations in rat visual cortex. Anesthesiology 102, 937–947.

Imas, O.A., Ropella, K.M., Wood, J.D., Hudetz, A.G., 2004. Halothane augments event-related gamma oscillations in rat visual cortex. Neuroscience 123, 269–278.

Janz, C., Heinrich, S.P., Kornmayer, J., Bach, M., Hennig, J., 2001. Coupling of neural activity and BOLD fMRI response: new insights by combination of fMRI and VEP experiments in transition from single events to continuous stimulation. Magn. Reson. Med. 46, 482–486.

Jenkinson, M., Bannister, P., Brady, M., Smith, S., 2002. Improved optimization for the robust and accurate linear registration and motion correction of brain images. NeuroImage 17, 825–841.

Kimura, D., 1962. Multiple response of visual cortex of the rat to photic stimulation. Electroencephalogr. Clin. Neurophysiol. 14, 115–122.

Kwong, K.K., Belliveau, J.W., Chesler, D.A., Goldberg, I.E., Weisskoff, R.M., Poncelet, B.P., Kennedy, D.N., Hoppel, B.E., Cohen, M.S., Turner, R., Cheng, H.-M., Brady, T.J., 1992. Dynamic magnetic resonance imaging of human brain activity during primary sensory stimulation. Proc. Natl. Acad. Sci. U. S. A. 89, 5675–5679.

Lee, J.G., Hudetz, A.G., Smith, J.J., Hillard, C.J., Bosnjak, Z.J., Kampine, J.P., 1994. The effects of halothane and isoflurane on cerebrocortical microcirculation and autoregulation as assessed by laser-Doppler flowmetry. Anesth. Analg. 79, 58–65.

Li, J., Wang, S., Bickford, M.E., 2003. Comparison of the ultrastructure of cortical and retinal terminals in the rat dorsal lateral geniculate and lateral posterior nuclei. J. Comp. Neurol. 460, 394–409.

Logothetis, N.K., Pauls, J., Augath, M., Trinath, T., Oeltermann, A., 2001. Neurophysiological investigation of the basis of the fMRI signal. Nature 412, 150–157.

Lu, H., Soltysik, D.A., Ward, B.D., Hyde, J.S., 2005. Temporal evolution of the CBV–fMRI signal to rat whisker stimulation of variable duration and intensity: a linearity analysis. NeuroImage 26, 432–440.

Ogawa, S., Lee, T.M., Kay, A.R., Tank, D.W., 1990. Brain magnetic resonance imaging with contrast dependent on blood oxygenation. Proc. Natl. Acad. Sci. U. S. A. 87, 9868–9872.

Ogawa, S., Lee, T.M., Stepnoski, R., Chen, W., Zhu, X.H., Ugurbil, K., 2000. An approach to probe some neural systems interaction by functional MRI at neural time scale down to milliseconds. Proc. Natl. Acad. Sci. U. S. A. 97, 11026–11031.

Ogawa, S., Tank, D.W., Menon, R., Ellermann, J.M., Kim, S.G., Merkle, H., Ugurbil, K., 1992. Intrinsic signal changes accompanying sensory stimulation: functional brain mapping with magnetic resonance imaging. Proc. Natl. Acad. Sci. U. S. A. 89, 5951–5955.

Paxinos, G., 2004. The Rat Nervous System, 3rd ed. Elsevier Academic Press, San Diego.

Paxinos, G., Watson, C., 2005. The Rat Brain in Stereotaxic Coordinates, 5th ed. Elsevier Academic Press, New York.

Riera, J.J., Watanabe, J., Kazuki, I., Naoki, M., Aubert, E., Ozaki, T., Kawashima, R., 2004. A state-space model of the hemodynamic approach: nonlinear filtering of BOLD signals. NeuroImage 21, 547–567.

Sloan, T.B., 1998. Anesthetic effects on electrophysiologic recordings. J. Clin. Neurophysiol. 15, 217–226.

Van Camp, N., Verhoye, M., De Zeeuw, C.I., Van der Linden, A., 2006a. Light stimulus frequency dependence of activity in the rat visual system as studied with high-resolution BOLD fMRI. J. Neurophysiol. 95, 3164–3170.

Van Camp, N., Verhoye, M., Van der Linden, A., 2006b. Stimulation of the rat somatosensory cortex at different frequencies and pulse widths. NMR Biomed. 19, 10–17.

Weber, R., Ramos-Cabrer, P., Wiedermann, D., van Camp, N., Hoehn, M., 2006. A fully noninvasive and robust experimental protocol for longitudinal fMRI studies in the rat. NeuroImage 29, 1303–1310.

Wyrwicz, A.M., Chen, N., Li, L., Weiss, C., Disterhoft, J.F., 2000. fMRI of visual system activation in the conscious rabbit. Magn. Reson. Med. 44, 474–478.

Yacoub, E., Ugurbil, K., Harel, N., 2006. The spatial dependence of the poststimulus undershoot as revealed by high-resolution BOLD- and CBV-weighted fMRI. J. Cereb. Blood Flow Metab. 26, 634–644.

Yesilyurt, B., Whittingstall, K., Ugurbil, K., Uludag, K., 2007. Insights into the dynamics of hemodynamic response to millisecond stimulus duration: an fMRI and VEP combination study. Proc. Int. Soc. Magn. Reson. Med. 15, 191.